Inorg. Chem. **1995,** *34,* 4305−4310

Synthesis and Structural Characterization of Niobium(IV) Amido Complexes and a Niobium(V) Bis(imido) Complex

Simon G. Bott,[1a] David M. Hoffman,*,[1b] and Sri Prakash Rangarajan[1b]

Departments of Chemistry, University of Houston, Houston, Texas 77204, and University of North Texas, Denton, Texas 76203

Received February 15, 1995[®]

$NbCl_4(thf)_2$ and 4 equiv of $LiNPh_2$ react to give the homoleptic Nb(IV) compound $Nb(NPh_2)_4$. The reactions of $NbX_4(thf)_2$ (X = Cl, Br) with 2 equiv of lithium bis(trimethylsilyl)amide lead to the Nb(IV) amido halide complexes $Nb(N(SiMe_3)_2)_2X_2$, but the reaction of $NbCl_4(PMe_3)_2$ with 2 equiv of $LiNH(2,6\text{-}C_6H_3\text{-}i\text{-}Pr_2)$ gives the Nb(V) bis(imido) complex $Nb(N\text{-}2,6\text{-}C_6H_3\text{-}i\text{-}Pr_2)_2Cl(PMe_3)_2$. A better preparation of the bis(imide) involves reacting $[Nb(NEt_2)_2Cl_3]_2$ sequentially with 2 equiv of $LiNH(2,6\text{-}C_6H_3\text{-}i\text{-}Pr_2)$ and PMe_3. Crystal data (Mo Kα radiation, $\lambda = 0.71073$ Å): $Nb(NPh_2)_4$, $C_{48}H_{40}N_4Nb$, T = −50 °C, $a = 10.596(3)$, $b = 11.622(4)$, $c = 16.177(5)$, $\alpha = 86.75(2)°$, $\beta = 80.63(2)°$, $\gamma = 80.33(3)°$, triclinic, space group $P\bar{1}$, Z = 2; $Nb(N(SiMe_3)_2)_2Br_2$, $C_{12}H_{36}Br_2N_2NbSi_4$, $a = 16.802(1)$ Å, $b = 8.7345(6)$ Å, $c = 20.388(2)$ Å, $\beta = 121.241(6)°$, monoclinic, space group $C2/c$, $Z = 4$; $Nb(N\text{-}2,6\text{-}C_6H_3\text{-}i\text{-}Pr_2)_2Cl(PMe_3)_2$, $C_{30}H_{52}ClN_2NbP_2$, $a = 17.1309(11)$ Å, $b = 9.6722(7)$ Å, $c = 20.7702(15)$ Å, $\beta = 95.934(6)$, monoclinic, space group $P2_1/c$, $Z = 4$.

Bradley and co-workers have synthesized the only known niobium(IV) homoleptic amides, $Nb(NR_2)_4$, where NR_2 = N-*n*-Bu_2, N-*n*-Pr_2, NEt_2, NMe_2, NC_5H_{10}, and NMe-*n*-Bu, and heteroleptic amides, $Nb(NEt_2)_3(NC_5H_{10})$, $Nb(NEt_2)_2(NC_5H_{10})_2$, and $Nb(NMe_2)(NEt_2)_3$.[2,3] The homoleptic amides were generally synthesized by reacting $LiNR_2$ with niobium pentachloride, and the heteroleptic compounds were prepared by transamination reactions. Whether niobium was reduced in the reactions of $NbCl_5$ with $LiNR_2$ depended upon the steric bulk and electron releasing ability of the amido ligand substituents. The only other reported Nb(IV) amide is $CpNb(NMe_2)_3$, which was synthesized from $Nb(NMe_2)_5$ and cyclopentadiene, but this compound was apparently not isolated in pure form.[4]

Because there are relatively few niobium(IV) amides and little is known about their chemistry, we were motivated to synthesize new derivatives. Also, on the basis of work by Fix et al., who used $Nb(NMe_2)_5$ and $Nb(NEt_2)_4$ to prepare Nb_3N_4 films,[5] we thought that the new Nb(IV) compounds might be viable precursors to niobium nitride films. In this paper, we describe the synthesis and characterization of $Nb(NPh_2)_4$, $Nb(N(SiMe_3)_2)_2Br_2$, and $Nb(N(SiMe_3)_2)_2Cl_2$.[6] We also describe $Nb(N\text{-}2,6\text{-}C_6H_3\text{-}i\text{-}Pr_2)_2Cl(PMe_3)_2$, a Nb(V) compound that was inadvertantly prepared during an attempt to synthesize a Nb(IV) aryl amide derivative.

Experimental Section

General Techniques. All manipulations were carried out in a glovebox or by using standard Schlenk techniques. The solvents, tetrahrahydrofuran, ether, hexane, and benzene, were distilled from Na/benzophenone. Acetonitrile was distilled from CaH_2. All solvents were stored in the drybox over 4-Å molecular seives. $NbCl_4L_2$ (L = thf or PMe_3),[7] $NbBr_4(thf)_2$[8] and $[Nb(NEt_2)_2Cl_3]_2$[9] were synthesized by the literature methods.

Elemental analyses were performed by Oneida Research Services, Whitesboro, NY. Infrared spectra were obtained for Nujol mulls between KBr plates in the 500−4000 cm^{-1} range by using a Mattson Galaxy 5000 FTIR. NMR spectra were collected on a GE 300-MHz instrument. Magnetic susceptibilities were determined for C_6D_6 solutions at room temperature by the Evans method using tetramethylsilane as the standard.[10,11] ^{31}P NMR spectra were collected on a Nicolet NT 300-MHz instrument for a toluene-d_8 solution.

$Nb(NPh_2)_4$. In the glovebox, $LiNPh_2$ (0.535 g, 3.16 mmol) was slowly added to a yellow suspension of $NbCl_4(thf)_2$ (0.3 g, 0.79 mmol) in ether (25 mL). The color of the solution gradually became very dark, almost black, after about 5 h. The solution was left to stir in the glovebox for 24 h. There was no further color change. The solution was then stripped to dryness, and the residue was extracted with benzene (2 × 10 mL). The extracts were filtered through Celite. The filtrate was stripped to dryness, and the residue was extracted with thf/CH_3CN (4:1, 1 × 20 mL). The extract was filtered through Celite, and the filtrate volume was then reduced to 8 mL. Black plates were formed by cooling at −36 °C for 24 h. The crystals were isolated by removing the mother liquor with a glass pipet and then were dried in vacuo (yield 0.38 g, 63%). Anal. Calcd for $C_{48}H_{40}N_4Nb$: C, 75.28; H, 5.26; N, 7.31. Found: C, 74.84; H, 5.35; N, 6.94. ^1H NMR (C_6D_6): δ 9.5 (broad). IR (cm^{-1}): 1587 m, 1308 w, 1255 m, 1242 m, 1184 m, 1172 m, 1026 w, 923 m, 873 m, 855 m, 748 m, 690 m.

$Nb(N(SiMe_3)_2)_2Br_2$. In the glovebox, $LiN(SiMe_3)_2$ (0.291 g, 1.74 mmol) was slowly added to a yellow suspension of $NbBr_4(thf)_2$ (0.50 g, 0.87 mmol) in hexane/ether (2:1, 20 mL). A series of color changes ensued, followed by the formation of a deep blue solution after ≈1 h. The solution was then stripped in vacuo, and the blue residue was extracted with hexane (1 x 10 mL). The extract was filtered through Celite. The blue filtrate was then reduced in volume to 5 mL. Blue plates formed by cooling the solution at −37 °C for 24 h. The crystals were isolated by removing the mother liquor with a glass pipet, and then were dried in vacuo (yield 0.27 g, 54%). Anal. Calcd for $C_{12}H_{36}Br_2N_2NbSi_4$: C, 25.13; H, 6.32; N, 4.88. Found: C, 26.68; H, 6.50;

[®] Abstract published in *Advance ACS Abstracts,* July 15, 1995.

(1) (a) University of North Texas. (b) University of Houston.

(2) Bradley, D. C.; Thomas, I. M. *Can. J. Chem.* **1962**, *40*, 449.

(3) Bradley, D. C.; Chisholm, M. H. *J. Chem. Soc. A* **1971**, 1511.

(4) Jenkins, A. D.; Lappert, M. F.; Srivastava, R. C. *J. Organomet. Chem.* **1970**, *23*, 165.

(5) Fix, R. M.; Gordon, R. G.; Hoffman, D. M. *J. Am. Chem Soc.* **1990**, *112*, 7833; *Chem. Mater.* **1993**, *5*, 614.

(6) A portion of this work has been communicated: Hoffman, D. M.; Rangarajan, S. P. *Polyhedron* **1993**, *12*, 2899.

(7) Manzer, L. E. *Inorg. Chem.* **1977**, *16*, 525.

(8) Pedersen, S. F.; Hartung, J. B., Jr.; Roskamp, E. J.; Dragovich, P. S. *Inorg. Synth.* **1992**, *29*, 119.

(9) Chao, Y.-W.; Polson, S.; Wigley, D. E. *Polyhedron* **1990**, *9*, 2709.

(10) Evans, D. F. *J. Chem. Soc.* **1959**, 2003.

(11) Live, D. H.; Chan, S. I. *Anal. Chem.* **1970**, *42*, 791.

0020-1669/95/1334-4305$09.00/0

N, 5.20. ^{1}H NMR (C_6D_6): δ 1.9 (broad). IR (cm^{-1}): 1253 s, 1170 w, 1112 w, 929 w, 850 vs, 785 s, 696 m, 667 s, 559 w, 505 w.

$Nb(N(SiMe_3)_2)_2Cl_2$. This compound was prepared from $NbCl_4(thf)_2$ following a procedure analogous to the one used to prepare the bromide derivative (blue plates; yield 0.37g, 59%). Anal. Calcd for $C_{12}H_{36}Cl_2N_2NbSi_4$: C, 29.74; H, 7.48; N, 5.78. Found: C, 30.88; H, 7.63; N, 5.80. ^{1}H NMR (C_6D_6): δ 1.9 (broad). IR (cm^{-1}): 1251 s, 1167 w, 1111 m, 961 m, 931 m, 835 s, 846 vs, 785 m, 767 w, 702 m, 669 m.

$Nb(N\text{-}2,6\text{-}C_6H_3\text{-}i\text{-}Pr_2)_2Cl(PMe_3)_2$. Method A. In a Schlenk flask, $LiNH(2,6\text{-}C_6H_3\text{-}i\text{-}Pr_2)$ (0.53 g, 2.92 mmol) was added to an orange-brown solution of $[Nb(NEt_2)_2Cl_3]_2$ (0.50 g, 0.73 mmol) in thf (20 mL). The color of the solution turned to light brown immediately. The solution was left to stir in the glovebox for 3 h, after which it was frozen in liquid nitrogen. PMe_3 (0.12 g, 1.68 mmol) was then condensed into the flask via a calibrated vacuum manifold. The mixture was slowly warmed to room temperature and then left to stir for 3 h. There was no further color change. The volatile components were removed in vacuo, and the brown residue was extracted with hexane (3 x 20 mL) and the extracts were filtered through Celite. The filtrate was stripped to dryness. The residue was then extracted with ether (20 mL), and the extract was filtered through Celite. Reducing the volume of the filtrate to 5 mL and then cooling the solution at −37 °C for 24 h yielded orange-red crystals, which were isolated by removing the supernatant solution with a pipet (yield 0.329 g, 42%). Anal. Calcd for $C_{30}H_{52}ClN_2NbP_2$: C, 57.09; H, 8.30; N, 4.43. Found: C, 56.97; H, 8.76; N, 4.51. ^{1}H NMR (C_6D_6): δ 7.17 (d, 4 H, *m*-H, N*Ar*), 7.01 (t, 2H, *p*-H, N*Ar*), 4.11 (sept, 4H, C*H*$(CH_3)_2$), 1.28 (d, J_{HH} = 6.6 Hz, 24H, CH(C*H*$_3$)$_2$), 1.15 (virtual t, 18H, P*Me*$_3$). $^{31}P\{^1H\}$ NMR (toluene-d_8) δ 160 (s). IR (cm^{-1}): 1587 w, 1525 w, 1421 s, 1336 s, 1280 m, 1259 s, 1153 w, 1105 w, 1018 w, 951 s, 885 w, 842 w, 802 w, 760 s, 748 s, 686 w, 603 m.

Method B. In the glovebox, $LiNH(2,6\text{-}C_6H_3\text{-}i\text{-}Pr_2)$ (0.35 g, 1.93 mmol) was added to an orange solution of $NbCl_4(PMe_3)_2$ (0.3 g, 0.96 mmol) in ether (20 mL). The color of the solution turned dark brown after stirring for 5 h. The solution was then stripped to dryness, and the brown residue was extracted with hexane (15 mL) and the extract was filtered through Celite. The volume of the filtrate was reduced to 5 mL. Cooling the solution at −37 °C for 24 h produced brown crystals, which were isolated by removing the supernatant solution with a pipet (yield 0.238 g, 39%).

X-ray Crystallography. Data was collected using graphite-monochromated Mo Kα radiation (λ = 0.710 73 Å). The data for $Nb(NPh_2)_4$ was collected at low temperature on a Nicolet R3m/V automatic diffractometer and then processed by using Nicolet's SHELXTL PLUS (1987) series of crystallographic programs. The data for $Nb(N(SiMe_3)_2)_2Br_2$ and $Nb(N\text{-}2,6\text{-}C_6H_3\text{-}i\text{-}Pr_2)_2Cl(PMe_3)_2$ were collected at room temperature on a Enraf-Nonius CAD-4F (κ geometry) diffractometer. Calculations were performed using the MolEN crystallographic software package. Details of the data collections and refinements are listed in Table 1, and atomic coordinates are listed in Tables 2−4.

$Nb(NPh_2)_4$. The crystals for study were grown from a cold saturated thf/CH_3CN solution (−37 °C). The thin purple-black plates were manipulated under mineral oil. The chosen crystal (0.44 × 0.24 × 0.04 mm) was rapidly transferred to the goniometer and then placed in a stream of cold nitrogen (−50 °C). The Laue symmetry was determined to be $\bar{1}$ and the space group was shown to be either $P1$ or $P\bar{1}$. Intensities were measured using the ω scan technique with the scan rate depending on the count obtained in rapid prescans of each deposition. During data reduction, Lorentz and polarization corrections were applied; however, no correction for absorption was made due to the small absorption coefficient.

The structure was solved by using the SHELXTL direct methods program, which revealed the positions of most of the non-hydrogen atoms in the molecule. Remaining atoms were found in subsequent difference Fourier syntheses. One of the phenyl groups (C(7)−C(12)) was found to be disordered over two slightly different positions. The disorder was treated by refining separate rigid bodies having 50% occupancy. After all shift/esd ratios were less than 0.1 (except for the rigid bodies) convergence was reached at the agreement factors listed in Table 1. No unsually high correlations were noted between any of the variables in the last cycle of full-matrix least-squares refinement, and the final difference density map showed a maximum peak of about 0.30 e/Å^3.

Table 1. Crystal Data Summaries for $Nb(NPh_2)_4$, $Nb(N(SiMe_3)_2)_2Br_2$, and $Nb(N\text{-}2,6\text{-}C_6H_3\text{-}i\text{-}Pr_2)_2Cl(PMe_3)_2$

	$Nb(NPh_2)_4$	$Nb(N(SiMe_3)_2)_2Br_2$	$Nb(NAr)_2Cl(PMe_3)_2$
empirical formula	$C_{48}H_{40}N_4Nb$	$C_{12}H_{36}Br_2N_2NbSi_4$	$C_{30}H_{52}ClN_2NbP_2$
fw	765.83	573.50	631.07
space group	$P\bar{1}$ (triclinic)	$C2/c$ (monoclinic)	$P2_1/c$ (monoclinic)
a, Å	10.596(3)	16.802(1)	17.1309(11)
b, Å	11.622(4)	8.7345(6)	9.6722(7)
c, Å	16.177(5)	20.388(2)	20.7702(15)
α, deg	86.75(2)		
β, deg	80.63(2)	121.241(6)	95.934(6)
γ, deg	80.33(3)		
temp, °C	−50	23	23
Z	2	4	4
V, Å^3	1937	2558	3423
D_{calcd}, g/cm^3	1.31	1.49	1.22
μ, cm^{-1}	3.33	37.28	5.26
R, R_w[a]	0.031, 0.027[b]	0.028, 0.028[c]	0.034, 0.046[c]

[a] $R = \sum||F_o| - |F_c||/\sum|F_o|$; $R_w = [\sum w(|F_o| - |F_c|)^2/\sum w|F_o|^2]^{1/2}$. [b] $w = \sigma(F)^{-2}$. [c] $w = [0.04F^2 + \sigma(F)^2]^{-1}$.

$Nb(N(SiMe_3)_2)_2Br_2$. The crystals for study were grown from a cold saturated hexane solution (−37 °C). A long blue block (0.40 × 0.45 × 0.90 mm) was mounted in a 0.7-mm o.d. Lindemann capillary under nitrogen. Intensities were measured by the ω scan technique. Three standard reflections were monitored after every 1 h of exposure time. Lorentz and polarization corrections were applied during data reduction. An absorption correction was applied (DIFABS). A Patterson map revealed the positions of the Nb atom. The remaining non-hydrogen atoms were located in subsequent difference Fourier syntheses. Hydrogen atoms were placed in calculated positions for refinement. No unusual problems were encountered during refinement, and the final difference map showed a maximum peak of 0.39 e/Å^3.

$Nb(N\text{-}2,6\text{-}C_6H_3\text{-}i\text{-}Pr_2)_2Cl(PMe_3)_2$. The crystals for study were grown from a cold saturated hexane solution (-37 °C). A red block (0.55 × 0.62 × 0.69 mm) was mounted in a 0.7-mm o.d. Lindemann capillary under nitrogen. Intensities were measured using the $\theta/2\theta$ scan technique. Three standard reflections were monitored after every 1 h of exposure time. Lorentz and polarization corrections were applied during data reduction. An absorption correction was applied (DIFABS). A Patterson map revealed the positions of the Nb atom. The remaining non-hydrogen atoms were located in subsequent difference Fourier syntheses. Hydrogen atoms were placed in calculated positions for refinement. No unusual problems were encountered during refinement, and the final difference map showed a maximum peak of 0.28 e/Å^3.

Results and Discussion

Synthesis and Characterization of $Nb(NPh_2)_4$. Thin purple-black plates of tetrakis(diphenylamido)niobium(IV), $Nb(NPh_2)_4$, were isolated in moderate yield by reacting $NbCl_4(thf)_2$[7] with 4 equiv of $LiNPh_2$ in ether, stripping and extracting with benzene, and crystallizing from thf/acetonitrile. The compound was also synthesized by reducing Nb(V) in situ; thus, the reaction of $NbBr_5$ with 4 equiv of $LiNPh_2$ and 2 equiv of Na/Hg gave $Nb(NPh_2)_4$ in 37% yield. A similar experiment using only 1 equiv of Na/Hg did not give crystals of $Nb(NPh_2)_4$, but the presence of a characteristic broad hump (see below) in the ^{1}H NMR spectrum of the stripped reaction mixture suggested the presence of the desired compound. $Nb(NPh_2)_4$ was also isolated in low yield (≈15%) by reacting $NbBr_5$ with 3 equiv of $LiNPh_2$ in ether, but the reaction was not reproducible. In this case, the $LiNPh_2$ must have acted as the reducing agent.

In the ^{1}H NMR spectrum of $Nb(NPh_2)_4$ (C_6D_6) only a single broad resonance at δ 9.5 is observed, implying the compound is paramagnetic. In the IR spectrum, $Nb(NPh_2)_4$ exhibits one

Table 2. Atomic Coordinates ($\times 10^4$) and Equivalent Isotropic Displacement Parameters ($Å^2 \times 10^3$) for $Nb(NPh_2)_4$

atom	*x*	*y*	*z*	*U*(eq)[a]
Nb	5995(1)	2575(1)	7449(1)	23(1)
N(1)	5422(3)	2340(3)	8696(2)	29(1)
N(2)	6185(3)	4288(3)	7349(2)	26(1)
N(3)	4741(3)	1957(3)	6830(2)	25(1)
N(4)	7682(3)	1664(3)	6960(2)	26(1)
C(1)	4177(4)	2697(3)	9166(2)	29(1)
C(2)	3087(4)	2882(3)	8766(3)	37(1)
C(3)	1875(4)	3285(4)	9193(3)	48(1)
C(4)	1700(4)	3520(4)	10037(3)	55(1)
C(5)	2768(4)	3341(4)	10439(3)	53(1)
C(6)	3987(4)	2931(4)	10021(3)	43(1)
C(7)	6476(4)	2065(4)	9148(3)	36(1)
C(8)	6585	986	9577	54(1)
C(9)	7653	602	9981	64(1)
C(10)	8612	1296	9957	54(1)
C(11)	8503	2375	9528	59(1)
C(12)	7436	2760	9123	48(1)
C(7′)	6368(4)	1735(3)	9185(3)	31(1)
C(8′)	6289	635	9563	48(1)
C(9′)	7264	83	10001	52(1)
C(10′)	8319	632	10062	38(1)
C(11′)	8398	1732	9683	43(1)
C(12′)	7423	2283	9245	39(1)
C(13)	4923(3)	4932(3)	7641(2)	26(1)
C(14)	3963(4)	5102(3)	7136(3)	30(1)
C(15)	2732(4)	5658(3)	7432(3)	40(1)
C(16)	2432(4)	6053(3)	8238(3)	45(1)
C(17)	3377(4)	5903(4)	8742(3)	47(1)
C(18)	4619(4)	5346(3)	8453(3)	38(1)
C(19)	7231(3)	4909(3)	7322(2)	27(1)
C(20)	7057(4)	6115(3)	7178(2)	31(1)
C(21)	8072(4)	6740(3)	7137(3)	38(1)
C(22)	9285(4)	6169(4)	7235(3)	43(1)
C(23)	9485(4)	4975(4)	7373(3)	43(1)
C(24)	8474(3)	4343(3)	7414(3)	34(1)
C(25)	4030(4)	2581(3)	6224(2)	27(1)
C(26)	4639(4)	3124(3)	5521(2)	38(1)
C(27)	3923(4)	3754(4)	4954(3)	49(1)
C(28)	2597(5)	3821(4)	5069(3)	56(1)
C(29)	1983(4)	3288(4)	5757(3)	61(1)
C(30)	2694(4)	2680(4)	6334(3)	42(1)
C(31)	4603(3)	745(3)	6938(2)	26(1)
C(32)	4563(4)	98(3)	6254(3)	48(1)
C(33)	4399(4)	−1063(4)	6355(3)	59(1)
C(34)	4286(4)	−1596(4)	7142(3)	49(1)
C(35)	4340(4)	−970(4)	7816(3)	45(1)
C(36)	4493(4)	202(3)	7719(3)	38(1)
C(37)	7989(3)	1743(3)	6054(2)	27(1)
C(38)	8141(4)	2786(3)	5638(3)	38(1)
C(39)	8404(4)	2840(4)	4769(3)	55(1)
C(40)	8532(4)	1855(4)	4321(3)	61(1)
C(41)	8392(4)	819(4)	4735(3)	58(1)
C(42)	8113(4)	748(4)	5595(3)	46(1)
C(43)	8594(4)	831(3)	7333(2)	28(1)
C(44)	9890(4)	956(3)	7201(3)	38(1)
C(45)	10806(4)	149(4)	7538(3)	50(1)
C(46)	10433(4)	−774(4)	8017(3)	50(1)
C(47)	9162(4)	−913(4)	8160(3)	50(1)
C(48)	8228(4)	−119(3)	7809(3)	39(1)

[a] Equivalent isotropic *U* defined as one-third of the trace of the orthogonalized $\mathbf{U}_{ij}$ tensor.

Table 3. Table of Positional Parameters and Equivalent Isotropic Displacement Parameters ($Å^2$) for $Nb(N(SiMe_3)_2)_2Br_2$

atom	*x*	*y*	*z*	*B*(eq)[a]
Nb	0.000	0.12854(8)	0.250	3.30(1)
Br	−0.12323(4)	−0.05595(8)	0.16463(3)	6.11(2)
Si(1)	−0.05808(9)	0.3799(2)	0.11997(7)	3.74(3)
Si(2)	0.10791(8)	0.1688(2)	0.15718(7)	3.74(3)
N	0.0231(2)	0.2379(5)	0.1777(2)	2.95(9)
C(11)	−0.1460(4)	0.4043(8)	0.1481(3)	5.6(2)
C(12)	−0.1234(4)	0.3161(8)	0.0178(3)	5.7(2)
C(13)	−0.0006(4)	0.5680(7)	0.1320(3)	5.8(2)
C(21)	0.2267(3)	0.1757(8)	0.2438(3)	5.8(2)
C(22)	0.0757(4)	−0.0283(8)	0.1199(3)	6.0(2)
C(23)	0.1144(4)	0.2839(9)	0.0838(3)	6.6(2)

[a] The isotropic equivalent displacement parameter is defined as (4/3)$\{a^2[B(1,1)] + b^2[B(2,2)] + c^2[B(3,3)] + ab(\cos\gamma)[B(1,2)] + ac(\cos\beta)[B(1,3)] + bc(\cos\alpha)[B(2,3)]\}$.

Table 4. Table of Positional Parameters and Equivalent Isotropic Displacement Parameters ($Å^2$) for $Nb(N\text{-}2,6\text{-}C_6H_3\text{-}i\text{-}Pr_2)_2Cl(PMe_3)_2$

atom	*x*	*y*	*z*	*B*(eq)[a]
Nb	0.20579(4)	0.03855(7)	0.36657(3)	2.99(1)
Cl	0.1349(1)	0.1910(2)	0.43893(9)	5.44(5)
P(1)	0.3042(1)	0.2471(3)	0.3875(1)	4.98(5)
P(2)	0.1061(1)	−0.1365(2)	0.4131(1)	4.96(5)
N(11)	0.2886(3)	−0.0771(6)	0.3886(2)	3.2(1)
N(21)	0.1750(3)	0.0462(6)	0.2801(2)	2.9(1)
C(1a)	0.3965(5)	0.235(1)	0.3524(5)	7.9(3)
C(1b)	0.2696(7)	0.421(1)	0.3691(6)	8.8(3)
C(1c)	0.3369(6)	0.258(1)	0.4721(5)	9.2(3)
C(2a)	0.1146(6)	−0.134(1)	0.5003(4)	7.9(3)
C(2b)	0.1202(7)	−0.318(1)	0.3947(6)	8.8(3)
C(2c)	0.0020(5)	−0.106(1)	0.3921(5)	8.1(3)
C(11)	0.3524(4)	−0.1659(8)	0.3960(3)	3.7(2)
C(12)	0.3944(4)	−0.1985(8)	0.3436(3)	3.9(2)
C(13)	0.4574(4)	−0.2906(9)	0.3539(4)	5.7(2)
C(14)	0.4789(5)	−0.348(1)	0.4127(4)	6.4(2)
C(15)	0.4396(5)	−0.314(1)	0.4634(4)	6.6(2)
C(16)	0.3771(4)	−0.2223(9)	0.4575(4)	5.2(2)
C(21)	0.1564(4)	0.0414(7)	0.2133(3)	3.2(1)
C(22)	0.1013(4)	−0.0564(7)	0.1847(3)	3.9(2)
C(23)	0.0803(5)	−0.0521(9)	0.1180(4)	5.8(2)
C(24)	0.1125(6)	0.042(1)	0.0791(4)	6.6(2)
C(25)	0.1654(5)	0.1333(9)	0.1068(4)	5.5(2)
C(26)	0.1895(4)	0.1369(7)	0.1725(3)	3.8(2)
C(121)	0.3701(4)	−0.1404(8)	0.2766(4)	5.0(2)
C(122)	0.4369(6)	−0.110(1)	0.2380(5)	9.1(3)
C(123)	0.3127(7)	−0.234(1)	0.2411(5)	9.6(3)
C(161)	0.3367(5)	−0.186(1)	0.5162(4)	7.6(3)
C(162)	0.3045(7)	−0.316(1)	0.5467(5)	10.4(4)
C(163)	0.3896(8)	−0.110(1)	0.5672(5)	12.1(4)
C(221)	0.0662(5)	−0.1649(9)	0.2237(4)	5.9(2)
C(222)	−0.0234(6)	−0.164(1)	0.2154(5)	9.3(3)
C(223)	0.0956(9)	−0.308(1)	0.2063(7)	12.3(5)
C(261)	0.2479(4)	0.2431(9)	0.1982(4)	4.8(2)
C(262)	0.3255(5)	0.228(1)	0.1704(5)	8.9(3)
C(263)	0.2172(6)	0.389(1)	0.1855(6)	9.3(3)

[a] The isotropic equivalent displacement parameter is defined as (4/3)$\{a^2[B(1,1)] + b^2[B(2,2)] + c^2[B(3,3)] + ab(\cos\gamma)[B(1,2)] + ac(\cos\beta)[B(1,3)] + bc(\cos\alpha)[B(2,3)]\}$.

medium intensity band at 690 cm^{-1} that may arise from the tetrahedral MN_4 group.[12,13] A medium intensity band at 1587 cm^{-1} is observed that can be assigned to the phenyl C−C stretch. The Evans NMR method[10,11] gives a room temperature magnetic moment of 0.98 μ_B, which is substantially lower than the spin only value of 1.73 μ_B. The low value is consistent, however, with the work of Bradley and Chisholm, who reported a magnetic moment of 0.8 μ_B for both $Nb(NEt_2)_4$ and $Nb(N\text{-}n\text{-}Pr_2)_4$.[3]

A thermal ellipsoid plot of $Nb(NPh_2)_4$ taken from an X-ray crystallographic study is shown in Figure 1. Selected bond distances and angles are given in Table 5. In $Nb(NPh_2)_4$ two opposite N−Nb−N angles [N(1)NbN(2) and N(3)NbN(4)] are small, averaging only 102°, and the planes defined by the two sets of atoms are twisted with respect to one another by 8°. The two small N−Nb−N angles and the twist cause the two other pairs of N−Nb−N angles to be significantly different,

---

(12) Nakamoto, K. *Infrared and Raman spectra of Inorganic and Coordination Compounds*, 4th ed.; John-Wiley & Sons: New York, 1986.

(13) Bradley, D. C.; Gitlitz, M. H. *J. Chem. Soc. A.* **1969**, 980.

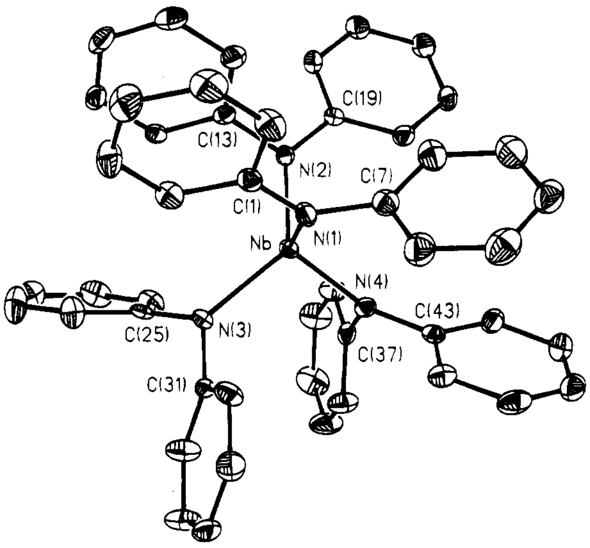

Figure 1. Plot of Nb(NPh$_2$)$_4$ showing the atom numbering scheme used in the tables (30% probability ellipsoids). Only one orientaton of the disordered phenyl ring (C(7)−C(12)) is shown.

Table 5. Selected Bond Distances (Å) and Angles (deg) for Nb(NPh$_2$)$_4$[a]

	Bond Distances		
Nb−N(1)	2.028(3)	Nb−N(2)	2.029(3)
Nb−N(3)	2.029(3)	Nb−N(4)	1.985(3)
N(1)−C(1)	1.420(4)	N(1)−C(7)	1.416(6)
N(2)−C(19)	1.415(5)	N(2)−C(13)	1.438(4)
N(3)−C(31)	1.438(5)	N(3)−C(25)	1.424(5)
N(4)−C(43)	1.430(5)	N(4)−C(37)	1.450(5)
	Bond Angles		
N(1)−Nb−N(2)	102.5(1)	N(1)−Nb−N(3)	108.2(1)
N(2)−Nb−N(3)	120.8(1)	N(1)−Nb−N(4)	116.7(1)
N(2)−Nb−N(4)	107.5(1)	N(3)−Nb−N(4)	101.9(1)
Nb−N(1)−C(1)	127.9(2)	Nb−N(1)−C(7)	112.8(2)
Nb−N(2)−C(13)	106.3(2)	Nb−N(2)−C(19)	134.8(2)
Nb−N(3)−C(25)	126.6(2)	Nb−N(3)−C(31)	119.2(2)
Nb−N(4)−C(37)	115.3(2)	Nb−N(4)−C(43)	131.2(2)
C(1)−N(1)−C(7)	117.1(3)	C(13)−N(2)−C(19)	115.4(3)
C(25)−N(3)−C(31)	114.0(3)	C(37)−N(4)−C(43)	113.1(3)

[a] Distances and angles are given for only one of the two orientations of the disordered phenyl ring (C(7)−C(12)). See the Supplementary Material for more details.

averaging 119° and 108°. The amido ligands are all close to planar, but the Nb−N−C angles vary widely (106−135°).

The Nb−N bond distances in Nb(NPh$_2$)$_4$ are unexceptional, being close, for example, to the mean basal Nb−N bond distances in Nb(NMe$_2$)$_5$ and Nb(NC$_5$H$_{10}$)$_5$ (average 2.042(15) Å and 2.052(14) Å respectively).[14] Interestingly, however, the Nb−N(4) distance in Nb(NPh$_2$)$_4$ is nearly 10σ shorter than the average of the other three statistically equal Nb−N distances. Comparing the four amido ligands, the sum of the Nb−N−C$_{ipso}$−C$_{ortho}$ torsion angles for the N(4) phenyl substituents is largest; that is, the blades of the two phenyls attached to N(4), when taken as a pair, are closest to being perpendicular to the Nb−N−C$_{ipso}$ plane than the other phenyl pairs. With this orientation, it is possible that N(4) can move closer to the metal while encountering less steric interaction.

The N(3) and N(4) amido ligand phenyl rings are rotated such that there is virtual C_2 symmetry in the Nb(N(3)Ph$_2$)(N(4)Ph$_2$) moiety, an arrangement that minimizes interligand steric interactions between rings. In contrast, the N(1) and N(2) phenyl substituents are oriented such that two of the rings [C(1) and C(13)] are in extremely close contact (≈3.2 Å), which would seem to maximize steric interactions.

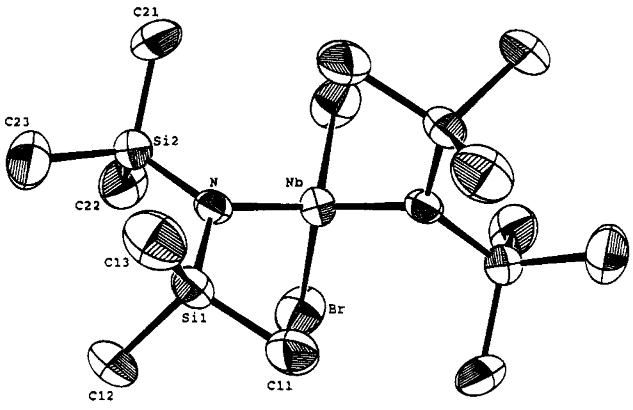

Figure 2. Plot of Nb(N(SiMe$_3$)$_2$)$_2$Br$_2$ showing the atom numbering scheme used in the tables (50% probability ellipsoids).

Table 6. Selected Bond Distances (Å) and Angles (deg) for Nb(N(SiMe$_3$)$_2$)$_2$Br$_2$

	Bond Distances		
Nb−Br	2.4849(7)	Si(1)−N	1.766(4)
Nb−N	1.957(4)	Si(2)−N	1.786(5)
	Bond Angles		
Br−Nb−Br′	99.08(7)	Br−Nb−N	101.98(9)
Br′−Nb−N	115.21(9)	N−Nb−N′	121.5(1)
Nb−N−Si(1)	117.3(2)	Nb−N−Si(2)	120.4(2)
Si(1)−N−Si(2)	121.0(2)		

Steric interactions are probably the reason why the structure of Nb(NPh$_2$)$_4$ is substantially distorted from tetrahedral. An indication of the steric congestion is the unusually wide variation in Nb−N−C angles. The distortions observed in the structure of Nb(NPh$_2$)$_4$ sharply contrast with the structure of d^2 Mo(NMe$_2$)$_4$, which has virtual D_{2d} symmetry with tetrahedral angles in the MoN$_4$ core.[15] In this regard, it should be noted that there is no apparent electronic driving force for the distortion in Nb(NPh$_2$)$_4$; a (d$_{x^2-y^2}$)^1 configuration is expected for Nb(NPh$_2$)$_4$,[15] giving Jahn−Teller inactive $^2B_1$ and ^2A ground states in D_{2d} and D_2 symmetries, respectively.

Synthesis and Characterization of Nb(N(SiMe$_3$)$_2$)$_2$Cl$_2$ and Nb(N(SiMe$_3$)$_2$)$_2$Br$_2$. Reaction of NbX$_4$(thf)$_2$ (X = Cl, Br)[7,8] with 2 equiv of lithium bis(trimethylsilyl)amide in hexane−ether, followed by stripping the solvent, extracting with hexane, and crystallizing from cold hexane, yields Nb(N(SiMe$_3$)$_2$)$_2$X$_2$ compounds as blue blocks. In both preparations there is ≈10% contamination of the final product by LiN(SiMe$_3$)$_2$. This has been difficult to remedy because of the similar solubilities of the lithium salt and niobium products. An attempt to sublime the lithium amide from the final product failed because the niobium amides decomposed at around 40 °C.

The ^{1}H NMR spectra of the Nb(N(SiMe$_3$)$_2$)$_2$X$_2$ compounds (C$_6$D$_6$) have only a broad resonance centered at approximately δ 1.9, implying they are paramagnetic. The Evans NMR method gives low room temperature magnetic moments of 1.03 and 0.98 μ_B for Nb(N(SiMe$_3$)$_2$)$_2$Cl$_2$ and Nb(N(SiMe$_3$)$_2$)$_2$Br$_2$, respectively.

A thermal ellipsoid plot for Nb(N(SiMe$_3$)$_2$)$_2$Br$_2$ is presented in Figure 2, and selected bond distances and angles are given in Table 6. The molecule has crystallographically imposed C_2 symmetry. The Br−Nb−Br′ angle is much smaller (99°) and the N−Nb−N′ much larger (121°) than 109.5°. Additionally,

---

(14) Heath, C.; Hursthouse, M. B. *J. Chem. Soc., Chem. Commun.* **1971**, 143.

(15) Chisholm, M. H.; Cotton, F. A.; Extine, M. W. *Inorg. Chem.* **1978**, *17*, 1329.

the $NbBr_2$ and NbN_2 planes are twisted by 9.4° with respect to one another, resulting in one Br−Nb−N angle being 13° larger than the other. The distortions from a tetrahedral geometry probably result from the steric congestion imposed by the bulky trimethylsilylamido groups. The coordination about the amido ligand nitrogen is essentially planar with the sum of the nearly equivalent angles being 359°.

The Nb-Br bond length (2.4849(7) Å) in $Nb(N(SiMe_3)_2)_2Br_2$ is comparable to the Nb-Br terminal distances in $[NbBr_4(\mu\text{-}Br)]_2$ (2.403(3), 2.462(2) Å).[16] The Nb−N bond length, 1.957(4) Å, is somewhat shorter than the Nb−N distances in $Nb(NPh_2)_4$, but it is considerably longer than the Nb−N multiple bond length in $Nb(NAr)_2Cl(PMe_3)_2$ (average 1.823(5), see below). The Si−N distances are close to the Si−N bond distances in $Ta(N(SiMe_3)_2)_2Cl_3$ (1.785−1.826(7) Å),[17] $Zr(N(SiMe_3)_2)_3Cl$ (1.766(3) and 1.766(4) Å) and $Hf(N(SiMe_3)_2)_3Cl$ (1.793(11) and 1.762(12) Å).[18]

An abbreviated X-ray cystallographic study of $Nb(N(SiMe_3)_2)_2Cl_2$ has been carried out.[6] It indicated that the space group and cell constants are virtually identical to those of $Ta(N(SiMe_3)_2)_2Cl_2$,[19] suggesting that the Nb and Ta compounds are isostructural.

Synthesis and Characterization of $Nb(N\text{-}2,6\text{-}C_6H_3\text{-}i\text{-}Pr_2)_2Cl(PMe_3)_2$. In an attempt to prepare a Nb(IV) aryl amido complex, the reaction of $NbCl_4(PMe_3)_2$[7] with 2 equiv of $LiNH(2,6\text{-}C_6H_3\text{-}i\text{-}Pr_2)$ in thf was carried out. Workup and crystallization from hexane gave yellow crystals of niobium(V) $Nb(N\text{-}2,6\text{-}C_6H_3\text{-}i\text{-}Pr_2)_2Cl(PMe_3)_2$ in 39% yield. The mechanism by which the Nb(V) complex forms probably involves a disproportionation reaction, but other pathways are also plausible. A more logical preparation of $Nb(N\text{-}2,6\text{-}C_6H_3\text{-}i\text{-}Pr_2)_2Cl(PMe_3)_2$ follows the work of Wigley et al., who synthesized the bis(imido) complexes $Nb(N\text{-}2,6\text{-}C_6H_3\text{-}i\text{-}Pr_2)_2Cl(py)_2$ and $Nb(N\text{-}2,4,6\text{-}C_6H_2Me_3)_2Cl(py)_2$ by reacting $[Nb(NEt_2)_2Cl_3]_2$[9] with 2 equiv of LiNHAr per niobium in thf, followed by the addition of pyridine.[20,21] Thus, the reaction of $[Nb(NEt_2)_2Cl_3]_2$ with 2 equiv of $LiNH(2,6\text{-}C_6H_3\text{-}i\text{-}Pr_2)$ per niobium in ether, followed by addition of PMe_3, produced yellow crystals of $Nb(N2,6\text{-}C_6H_3\text{-}i\text{-}Pr_2)_2Cl(PMe_3)_2$ in 42% yield after extraction with hexane and crystallization from ether.

Proton NMR spectra for $Nb(N\text{-}2,6\text{-}C_6H_3\text{-}i\text{-}Pr_2)_2Cl(PMe_3)_2$ display characteristic resonances for the isopropyl and phenyl protons of the aryl moiety, and a virtual triplet for the *trans*-PMe_3 ligands at δ 1.15. The $^{31}P\{^1H\}$ NMR spectrum at room temperature shows a sharp singlet at δ 160.

A thermal ellipsoid plot of $Nb(N\text{-}2,6\text{-}C_6H_3\text{-}i\text{-}Pr_2)_2Cl(PMe_3)_2$ is presented in Figure 3, and selected bond distances and angles are presented in Table 7. The distorted trigonal bipyramidal structure of $Nb(N\text{-}2,6\text{-}C_6H_3\text{-}i\text{-}Pr_2)_2Cl(PMe_3)_2$ is similar to that of $Ta(N\text{-}2,6\text{-}C_6H_3\text{-}i\text{-}Pr_2)_2Cl(py)_2$.[20] The average length of the Nb−N bonds (average 1.823(5)), which are best described as having bond order 2.5, is comparable to the Nb−N bond length (1.89(1) Å) in $[Li(THF)_2]_2[Nb(N\text{-}2,4,6\text{-}C_6H_2Me_3)_3(n\text{-}Bu)]$,[21] though it is longer, for example, than the niobium−imido bond lengths in $[Nb(\mu\text{-}Cl)Cl_2(Me_2S)(NC_6H_5)]_2$[22] (1.733(7) Å) and $[Nb(\eta\text{-}C_5H_5)(N\text{-}2,6\text{-}C_6H_3\text{-}i\text{-}Pr_2)(PMe_3)(C_3H_6)]$ (1.793(11) Å).[23]

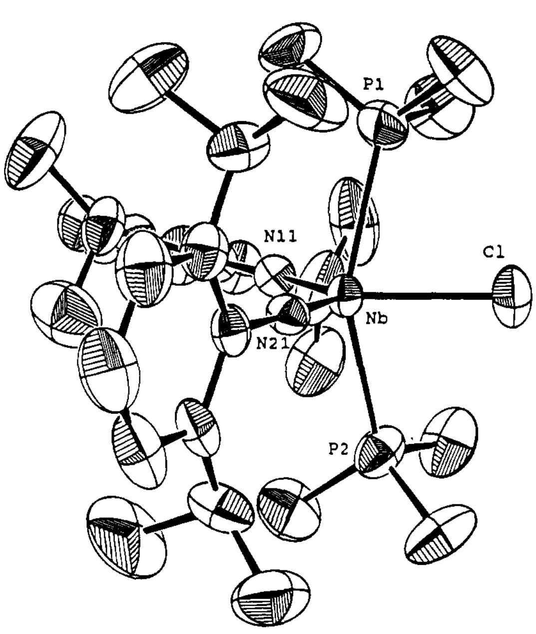

Figure 3. Plot of $Nb(N\text{-}2,6\text{-}C_6H_3\text{-}i\text{-}Pr_2)_2Cl(PMe_3)_2$ showing the atom numbering scheme used in the tables (30% probability ellipsoids).

Table 7. Selected Bond Distances (Å) and Angles (deg) for $Nb(N\text{-}2,6\text{-}C_6H_3\text{-}i\text{-}Pr_2)_2Cl(PMe_3)_2$

	Bond Distances		
Nb-Cl	2.507(2)	Nb−N(21)	1.819(5)
Nb−P(1)	2.636(2)	N(11)−C(11)	1.385(8)
Nb−P(2)	2.656(2)	N(21)−C(21)	1.391(7)
Nb−N(11)	1.827(5)		
	Bond Angles		
Cl−Nb−P(1)	78.04(7)	Cl−Nb−P(2)	77.72(7)
Cl−Nb−N(11)	128.5(2)	Cl−Nb−N(21)	117.3(2)
P(1)−Nb−N(11)	87.7(2)	P(2)−Nb−N(11)	91.7(2)
P(1)−Nb−N(21)	104.3(2)	P(2)−Nb−N(21)	104.6(2)
P(1)−Nb−P(2)	148.45(7)	N(11)−Nb−N(21)	114.2(2)

The imido ligands are nearly linear (average Nb−N−C = 173°), as they are in $Ta(N\text{-}2,6\text{-}C_6H_3\text{-}i\text{-}Pr_2)_2Cl(py)_2$ (∠Ta−N−C = 170.9(5)° and 165.4(5)°).[20] To avoid steric interactions between the Ph groups, one of the phenyls (C(21)−C(26)) is oriented such that it lies nearly in the $NbClN_2$ trigonal plane (∠ between planes = 19°) and the other is nearly perpendicular to the plane (88°). A similar orientation of the imido ligands is also observed in $Ta(N\text{-}2,6\text{-}C_6H_3\text{-}i\text{-}Pr_2)_2Cl(py)_2$. The PMe_3 ligands are severely bent away from the imides (P(1)-Nb-P(2) = 148.45(7)°), as is common for ligands that are cis to multiply bonded atoms in d^0 complexes. There are also two sets of disparate N-Nb-P angles that apparently result from steric repulsion between the PMe_3 ligands and the *i*-Pr groups groups on the C(21) phenyl ring.

Conclusion

The homoleptic Nb(IV) amido complex $Nb(NPh_2)_4$ and Nb(IV) amido halide complexes $Nb(N(SiMe_3)_2)_2X_2$ (X = Cl and Br) are prepared from $NbX_4(thf)_2$ in moderate yields by salt metathesis reactions. X-ray crystallographic studies of $Nb(N(SiMe_3)_2)_2Br_2$ and $Nb(NPh_2)_4$ show that they both have distorted tetrahedral geometries in the solid state, presumably resulting from steric congestion due to the bulky amido ligands. $Nb(N(SiMe_3)_2)_2Br_2$ and $Nb(NPh_2)_4$ appear to be the first structurally characterized examples of Nb(IV) amido compounds.

---

(16) Müller, U.; Klingelhöfer, P. *Z. Naturforsch., B* **1983**, *38*, 559.
(17) Bradley, D. C.; Hursthouse, M. B.; Malik, K. M. A.; Vuru, G. B. C. *Inorg. Chim. Acta.* **1980**, *44*, L5.
(18) Airoldi, C.; Bradley, D. C., Chudzynska, H.; Hursthouse, M. B.; Malik, K. M. A.; Raithby, P. R. *J. Chem. Soc., Dalton Trans.* **1980**, 2010.
(19) Hoffman, D. M.; Suh, S. *J. Chem. Soc., Chem. Commun.* **1993**, 714.
(20) Chao, Y.-W.; Wexler, P. A.; Wigley, D. E. *Inorg. Chem.* **1990**, *29*, 4592.
(21) Smith, D. P.; Allen, K. D.; Carducci, M. D.; Wigley, D. E. *Inorg. Chem.* **1992**, *31*, 1319.
(22) Cotton, F. A.; Duraj, S. A.; Roth, W. J. *J. Am. Chem. Soc.* **1984**, *106*, 4749.
(23) Poole, A. D.; Gibson, V. C.; Clegg, W. *J. Chem. Soc., Chem. Commun.* **1992**, 237.

The reaction of $NbCl_4(PMe_3)_2$ with 2 equiv of $LiNH(2,6\text{-}C_6H_3\text{-}i\text{-}Pr_2)$ gives the Nb(V) bis(imido) complex $Nb(N\text{-}2,6\text{-}C_6H_3\text{-}i\text{-}Pr_2)_2Cl(PMe_3)_2$. Following the work of Wigley et al.,[20,21] the bis(amide) is more logically prepared by reacting $[Nb(NEt_2)_2Cl_3]_2$ with $LiNH(2,6\text{-}C_6H_3\text{-}i\text{-}Pr_2)$ followed by the addition of PMe_3. The X-ray structure of $Nb(N\text{-}2,6\text{-}C_6H_3\text{-}i\text{-}Pr_2)_2Cl(PMe_3)_2$ shows that it has a distorted trigonal bipyramidal structure that is similar to $Ta(N\text{-}2,6\text{-}C_6H_3\text{-}i\text{-}Pr_2)_2Cl(py)_2$.

Acknowledgment for support is made to the Petroleum Research Fund, administered by the American Chemical Society, and the Robert A. Welch Foundation. D.M.H. is a 1992–1994 Alfred P. Sloan Research Fellow. We are grateful to J. Korp for his technical assistance with the X-ray crystallographic analysis of $Nb(NPh_2)_4$ and his helpful discussions.

Supporting Information Available: Tables of crystal data, atomic coordinates, thermal parameters, bond lengths and angles, least squares plane; plots and packing diagrams for $Nb(NPh_2)_4$, $Nb(N(SiMe_3)_2)_2Br_2$, and $Nb(N\text{-}2,6\text{-}C_6H_3\text{-}i\text{-}Pr_2)_2Cl(PMe_3)_2$ (49 pages). Ordering information is given on any current masthead page. Tables of observed and calculated structure factors can be obtained from the authors.

IC9501834